

Boundary of Nuclear Physics and QCD

A. W. Thomas

*Department of Physics and Mathematical Physics and
Special Research Centre for the Subatomic Structure of Matter
The University of Adelaide, Adelaide SA 5005, Australia*

Abstract. Recent progress in lattice QCD, combined with the imminent advent of a new generation of dedicated supercomputers and advances in chiral extrapolation mean that the next few years will bring quite novel insights into hadron structure. We review some of the recent highlights in this field, the questions which might be addressed and the experiments which may be expected to stretch that understanding to its limits. Only with a sound understanding of hadron structure can one hope to explore the fundamental issue of how that structure may change at finite density (or temperature). We explore potential future insights from lattice QCD into the phenomenon of nuclear saturation and a very important hint from recent data of a change in the structure of a bound nucleon.

INTRODUCTION

Modern nuclear physics presents a wonderfully exciting and diverse set of challenges. Perhaps the most fundamental of these is the challenge to understand nuclear phenomena in terms of the underlying theory of the strong interaction - Quantum Chromodynamics or QCD. At this meeting we saw some excellent discussions of QCD at high temperature (T) and density (ρ), especially in the context of relativistic heavy ion collisions, the quark-gluon plasma and beyond. We concentrate on the lower density regime which is generally termed hadronic physics. This is the other sector of nuclear physics which can naturally be addressed in terms of QCD.

Hadronic physics is currently at an extremely exciting stage of development. New experimental capabilities at laboratories such as JLab, Mainz and MIT-Bates are extending our knowledge of nucleon form factors free and bound (as well as transition form factors) into new kinematic domains and with unheard of precision. We are beginning to see the development of phenomenologically meaningful, covariant models of hadron structure and these can be extended to incorporate chiral symmetry. With the development of clever improved actions, faster computers and better treatments of chiral symmetry, lattice QCD is soon to deliver on its promise of deep new insights into hadron structure. Indeed, as we shall describe, in combination with carefully controlled chiral extrapolation one can expect to calculate accurate properties of the low mass baryons within a few years. One can also hope to rigorously address some key physics issues in hadron spectroscopy.

In the decade since Brown and Rho focused attention on the possible change of hadron properties in-medium, the topic has generated enormous theoretical and experimental interest. We briefly outline the role of changes of nucleon internal structure within relativistic mean field theory. We also suggest how lattice input might feed directly into such calculations. Finally, we report on what has the potential to be a very important development in this field, namely the recent determination of G_E/G_M for a proton bound in ^4He . The relative insensitivity of the analysis to various theoretical corrections, combined with the apparent deviation from the free G_E/G_M ratio, will stimulate a great deal of interest. In the context of understanding nuclear structure in terms of QCD, it is the first firm evidence for the change in the structure of a bound nucleon which must be there.

¹ Invited presentation at the International Conference on Nuclear Physics (INPC2001): Berkeley, July 30 to August 3, 2001
University of Adelaide preprint: ADP-01-32/T464

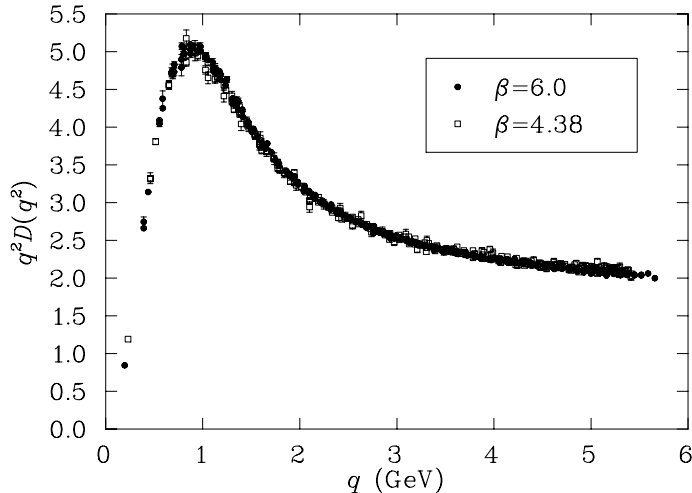


FIGURE 1. Non-perturbative behaviour of the gluon propagator (times q^2) in Landau gauge, calculated from lattice QCD – from Ref. [10].

In the next section we make some general remarks about QCD, its bizarre properties and the nature of the QCD vacuum. After describing recent advances in linking lattice QCD to covariant models of hadron structure we summarise the crucial issue of chiral extrapolation. The recent progress in this area, for which we present several examples, underpins the exciting prospect that we may be able to calculate accurate hadronic properties at the physical quark mass in just a few years. We close the discussion with an outlook of the recent progress in hadron spectroscopy. The third section deals with the in-medium properties of hadrons, while the final section contains some closing remarks.

LATTICE QCD AND HADRON STRUCTURE

The bizarre properties of QCD are well known. It exhibits asymptotic freedom at short distances while it is confining in the long distance regime. At least qualitatively one can understand confinement in terms of non-trivial QCD vacuum structure – essentially a dual superconductor [1]. This confines the colour electric fields (dual to the magnetic fields in the case of a normal superconductor) between quarks into a flux tube of approximately constant area. Hence the energy to separate two quarks grows linearly with separation. To put the forces being discussed into context, it is worth noting that the rate of growth of the energy, the string tension, is approximately 1 GeV/fm ($\sigma = (440 \text{ MeV})^2$). This corresponds to a constant, confining force of order 10 tonnes – a force characteristic of trucks acting between objects less than 10^{-18}m in size!

The non-trivial nature of the QCD vacuum is illustrated by the fact that it contains both quark and gluon condensates [2]. For a purely gluonic version of QCD the vacuum energy density, ϵ_{vac} , is [3]:

$$\epsilon_{\text{vac}} = -\frac{9}{32} \langle 0 | \frac{\alpha_s}{\pi} G^2 | 0 \rangle = -0.5 \text{ GeV}/\text{fm}^3. \quad (1)$$

In comparison with phenomenological estimates of the energy difference between the perturbative and non-perturbative vacuum states, such as B in the MIT bag model, this is an order of magnitude larger. Thus, either the popular idea of the perturbative vacuum being fully restored inside a hadron is incorrect or the situation is rather more complicated than commonly assumed.

These gluon fields in vacuum also show important topological structure, such as the famous instantons [4]. This topology is believed to be connected with chiral symmetry breaking, which we will consider soon. For the present we note that current lattice simulations allow us to actually display this topological structure, to correlate it with regions of high action density and to examine its development in Euclidean time. It is impossible to display such information here, but the interested reader is referred to various animations, generated by Leinweber and collaborators, on the CSSM web pages [5] (see also Ref. [6]). At first glance it is clear that the topological structures are neither spherical nor weakly interacting, but the benefits of these visualizations are just beginning to be appreciated.

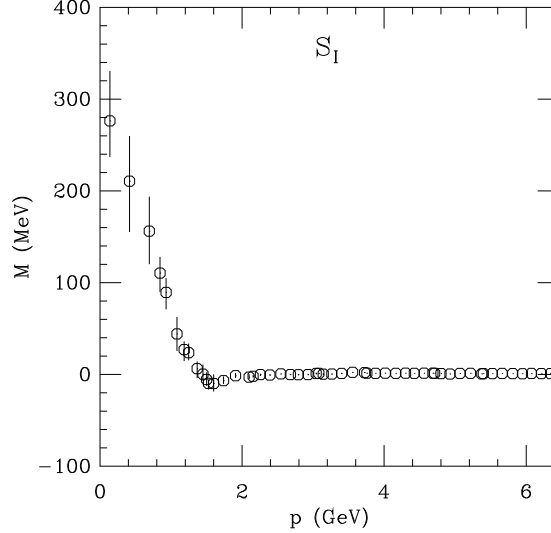


FIGURE 2. Non-perturbative behaviour of the quark mass function, $M(p^2)$, extrapolated linearly to the chiral limit, on the basis of lattice QCD simulations – from Ref. [14].

Covariant models of hadron structure are very much in their infancy. Nevertheless, substantial progress has been made in understanding the structure of the low-lying pseudoscalar and vector mesons within a phenomenological implementation of the Dyson-Schwinger equations [7, 8]. In addition, there have been some promising developments in the baryon sector based on the Faddeev equations [9]. Until now the phenomenological input has been chosen to reproduce some limited set of experimental data and then applied to other problems. However, the sophistication of modern lattice gauge theory is such that one can now begin to check key parts of these covariant calculations against lattice simulations.

The natural starting point for comparisons between covariant calculations and lattice simulations are the quark and gluon propagators. The long term aim is to refine the model building process using QCD itself. Of course, intermediate steps such as the quark and gluon propagators are not physical and one must specifically fix the gauge in order to make a meaningful comparison. The gauge most commonly used is Landau gauge and techniques have been developed to fix lattice quantities in this gauge. Figure 1 shows the result for the non-trivial momentum dependence of the gluon propagator (times q^2) [10], $q^2 D(q^2)$, which should go to a constant at large q^2 (up to perturbative QCD logs). From Fig. 1 we see that the lattice simulation shows that the gluon propagator is clearly *non-perturbative* for $q^2 < 4\text{GeV}^2$. Even more interesting from the point of view of model building is the fact that the gluon propagator is not enhanced as $q^2 \rightarrow 0$. While this agrees with some recent Schwinger-Dyson studies of QCD [11], it is in disagreement with at least a naive interpretation of a great deal of phenomenological work related to dynamical chiral symmetry breaking within that formalism [12]. Clearly this sort of interplay between phenomenological models and QCD itself has just begun and we have a great deal to learn from it.

Again with Landau gauge fixing, there have been some preliminary studies of the quark propagator in QCD. For Euclidean p^2 one can write the quark propagator as:

$$S_E(p) = \frac{Z(p^2)}{i\gamma_\mu p_\mu + M(p^2)}. \quad (2)$$

The lattice simulations, which have so far been carried out with relatively large current quark masses, show a clear enhancement in the infrared [13, 14]. For example, for a current quark mass of order 110 MeV, the simulations suggest $M(0) \sim 400$ MeV, decreasing to around 300 MeV in the chiral limit. We illustrate the mass function, $M(p^2)$, in the chiral limit, as calculated by Leinweber et al. [14], in Fig. 2. The enhancement in the infrared region, leading to a quark effective mass of order 300 MeV, is clearly consistent with the general idea of the constituent quark model. Indeed this result provides a firm theoretical foundation for the concept within QCD. Of course, it also indicates where the concept breaks down and it is clear that in processes involving significant momentum transfer it will be necessary to go beyond the simple idea of a fixed mass. The similarity of the mass function, $M(p^2)$, to that found in Schwinger-Dyson studies suggests that the latter may be a promising phenomenological extension of the constituent quark idea.

One of the crucial tests of QCD itself is the quest for hadrons in which gluons play a genuine structural role. For example, the experimental discovery of exotic mesons, where the quantum numbers cannot be associated with a $q\bar{q}$ pair alone, would be a vital step towards a full understanding of QCD. This explains the excitement over the announcement, from E852 at Brookhaven National Lab [15], of three candidates for hybrid mesons with quantum numbers $J^{PC} = 1^{-+}$. The $\pi'(1370)$ was seen in the $\pi\eta$ and $\pi\eta'$ channels, the $\pi'(1640)$ in $\pi\eta'$, $\rho\pi$ and $f_1\pi$ and the $\pi'(2000)$ in $a_1\eta$. These masses are somewhat lower than the values usually reported in lattice simulations, although for the moment the latter tend to be based on quenched QCD [16, 17]. While the interpretation of the BNL data should become clearer over the next few years, the announcement lends even greater urgency to the calls for a future HALL D program at Jefferson Lab [18].

An even more dramatic prediction of QCD than exotic states is, of course, the possibility of physical particles containing *only* glue – the glueballs. Lattice simulations suggest that the lowest mass state of pure glue would be the 0^{++} with a mass of $1611 \pm 30 \pm 160$ MeV [19]. Experimental searches have so far found a number of scalar glueball candidates in the mass region 1300 to 1800 MeV [20]. However, the interpretation of the data is badly effected by the fact that in *real* QCD, with light quarks, no physical state will be pure glue – rather the best one can hope for is an unstable state with only a small $q\bar{q}$ component for some (unknown) dynamical reason. We note that the channel coupling effects induced by decay channels such as $\pi\pi$ and $K\bar{K}$ are also quite controversial from the theoretical point of view. There is clearly room for a great deal of experimental and theoretical work in this field in the future.

Chiral Symmetry in the Context of Lattice QCD

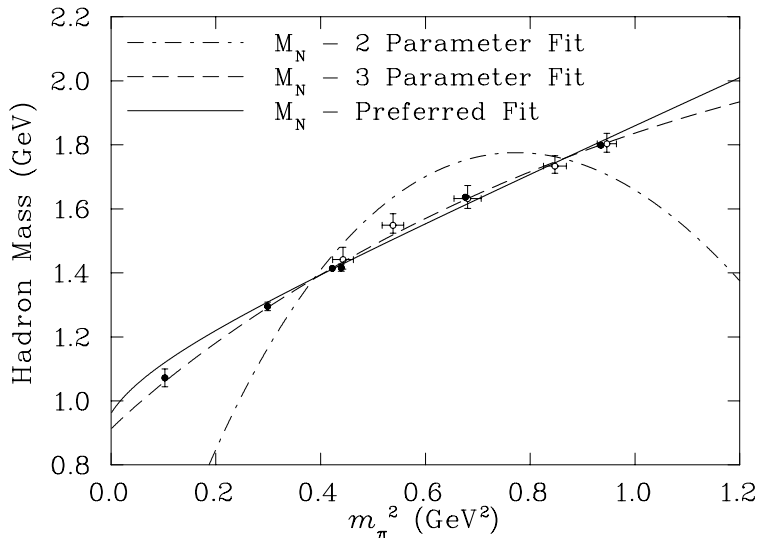


FIGURE 3. A comparison between phenomenological fitting functions for the mass of the nucleon – from Ref. [21]. The two parameter fit corresponds to using Eq.(5) with γ set equal to the value known from χ PT. The three parameter fit corresponds to letting γ vary as an unconstrained fit parameter. The solid line is the two parameter fit based on the functional form of Eq.(6).

The essential problem in performing calculations at realistic quark masses (of order 5 MeV) is the approximate chiral symmetry of QCD. Goldstone’s theorem tells us that chiral symmetry is dynamically broken and that the non-perturbative vacuum is highly non-trivial, with massless Goldstone bosons in the limit $\bar{m} \rightarrow 0$ [2]. For finite quark mass these bosons are the three charge states of the pion with a mass $m_\pi^2 \propto \bar{m}$. Although this result strictly holds only for m_π^2 near zero (the Mann-Oakes-Renner relation), lattice simulations show it is a good approximation for m_π^2 up to 0.8 GeV^2 and we shall use m_π^2 as a measure of the deviation from the chiral limit.

From the point of view of lattice simulations with dynamical quarks (i.e. unquenched) the essential difficulty is that the time taken goes as \bar{m}^{-3} , or worse [22]. The state-of-the-art for hadron masses is \bar{m} above 60 MeV, although there is a preliminary result from CP-PACS at about 40 MeV [23]. In general the quark masses for which simulations currently exist are at masses a factor of 8-20 too high. This means that an increase of computing power to several hundred tera-flops is needed if one is to calculate realistic hadron properties. Even with the current remarkable rate of increase this will take a long time.

Faced with such a serious difficulty physicists (like all other people facing a tough challenge) fall into two classes:
 (A) Those who believe that “the cup is half empty”:

In this case the emphasis is on the uncertainties associated with having to make big extrapolations to the chiral limit.

(B) Those who believe that “the cup is half full”:

In this case we realize that the lattice data obtained so far represents a wealth of information on the properties of hadrons within QCD itself over a range of quark masses. Just as the study of QCD as a function of N_c has taught us a great deal, so the behaviour as a function of \bar{m} can give us great insight into hadronic physics and guide our model building. Furthermore, as a bonus, approach (B) leads us to resolve most of the difficulty identified under (A)!

In light of the brief space available to outline a great deal of evidence we first summarise the conclusions which emerge from the work of the past three years. We then present several illustrations of the reasoning which led to these conclusions.

Summary:

- In the region of quark masses $\bar{m} > 60$ MeV or so (m_π greater than typically 400-500 MeV) hadron properties are smooth, slowly varying functions of something like a constituent quark mass, $M \sim M_0 + c\bar{m}$ (with $c \sim 1$).
- Indeed, $M_N \sim 3M, M_{p,\omega} \sim 2M$ and magnetic moments behave like $1/M$.
- As \bar{m} decreases below 60 MeV or so, chiral symmetry leads to rapid, non-analytic variation, with:
 $\delta M_N \sim \bar{m}^{3/2}$,
 $\delta \mu_H \sim \bar{m}^{1/2}$,
 $\delta < r^2 >_{\text{ch}} \sim \ln \bar{m}$ and
 moments of non-singlet parton distributions $\sim m_\pi^2 \ln m_\pi$.
- Chiral quark models, like the cloudy bag model (CBM) [24], provide a natural explanation of this transition. The scale is basically set by the inverse size of the pion source – the inverse of the bag radius in the CBM.
- When the pion Compton wavelength is smaller than the size of the composite source chiral loops are strongly suppressed. On the other hand, as soon as the pion Compton wavelength is larger than the source one begins to see rapid, non-analytic chiral corrections.

The nett result of this discovery is that one has control over the chiral extrapolation of hadron properties provided one can get data at pion masses of order 200–300 MeV. This seems feasible with the next generation of supercomputers which should be available within 2–3 years and which will have speeds in excess of 10 tera-flops [25]. This is an extremely exciting possibility in that it will bring the scale of realistic calculations of physical hadron properties by a decade or more!

Chiral Loops and Non-Analyticity

We have already seen that spontaneous chiral symmetry breaking in QCD requires the existence of Goldstone bosons whose masses vanish in the limit of zero quark mass (the chiral limit). As a corollary to this, there must be contributions to hadron properties from Goldstone boson loops. These loops have the unique property that they give rise to terms in an expansion of most hadronic properties as a function of quark mass which are not analytic [26]. As a simple example, consider the nucleon mass. The most important chiral corrections to M_N come from the processes $N \rightarrow N\pi \rightarrow N$ (σ_{NN}) and $N \rightarrow \Delta\pi \rightarrow N$ ($\sigma_{N\Delta}$). We write $M_N = M_N^{\text{bare}} + \sigma_{NN} + \sigma_{N\Delta}$. In the heavy baryon limit one has

$$\sigma_{NN} = -\frac{3g_A^2}{16\pi^2 f_\pi^2} \int_0^\infty dk \frac{k^4 u^2(k)}{k^2 + m_\pi^2}. \quad (3)$$

Here $u(k)$ is a natural high momentum cut-off which is the Fourier transform of the source of the pion field (e.g. in the CBM it is $3j_1(kR)/kR$, with R the bag radius [24]). From the point of view of PCAC it is natural to identify $u(k)$ with the axial form-factor of the nucleon, a dipole with mass parameter $1.02 \pm 0.08\text{GeV}$ [2].

Totally independent of the form chosen for the ultra-violet cut-off, one finds that σ_{NN} is a non-analytic function of the quark mass. The non-analytic piece of σ_{NN} is independent of the form factor and gives

$$\sigma_{NN}^{LNA} = -\frac{3g_A^2}{32\pi f_\pi^2} m_\pi^3 \sim \bar{m}^{3/2}. \quad (4)$$

This has a branch point, as a function of \bar{m} , starting at $\bar{m} = 0$. Such terms can only arise from Goldstone boson loops.

It is natural to ask how significant this non-analytic behaviour is in practice. If the pion mass is given in GeV, $\sigma_{NN}^{LNA} = -5.6m_\pi^3$ and at the physical pion mass it is just -17 MeV. However, at only three times the physical pion mass, $m_\pi = 420\text{MeV}$, it is -460MeV – half the mass of the nucleon. If one’s aim is to extract physical nucleon properties from lattice QCD calculations this is extremely important. As we explained earlier, the most sophisticated lattice calculations with dynamical fermions are only just becoming feasible at such low masses and to connect to the physical world one must extrapolate from $m_\pi \sim 500\text{MeV}$ to $m_\pi = 140\text{MeV}$. Clearly one must have control of the chiral behaviour. Figure 3 shows recent lattice calculations of M_N as a function of m_π^2 from CP-PACS and UKQCD [23, 27]. The dashed line indicates a fit which naively respects the presence of a LNA term,

$$M_N = \alpha + \beta m_\pi^2 + \gamma m_\pi^3, \quad (5)$$

with α, β and γ fitted to the data. While this gives a very good fit to the data, the chiral coefficient γ is only -0.761, compared with the value -5.60 required by chiral symmetry. If one insists that γ be consistent with QCD the best fit one can obtain with this form is the dash-dot curve. This is clearly unacceptable.

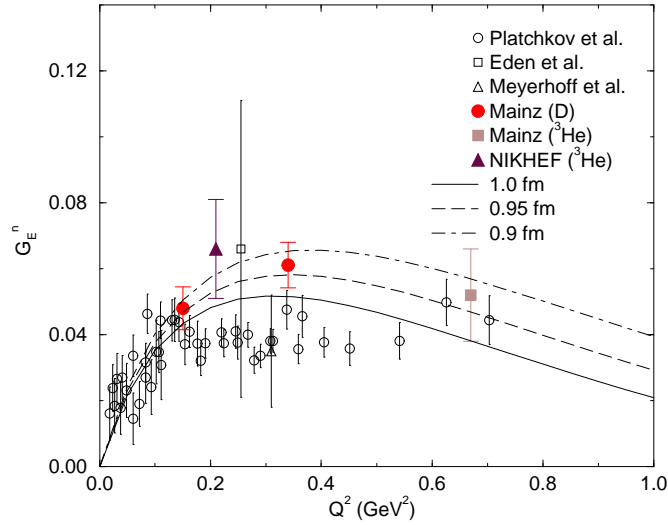


FIGURE 4. Recent data for the neutron electric form factor in comparison with CBM calculations for a confining radius around 0.95fm – from Ref. [34].

An alternative suggested recently by Leinweber et al. [21], which also involves just three parameters, is to evaluate σ_{NN} and $\sigma_{N\Delta}$ with the same ultra-violet form factor, with mass parameter Λ , and to fit M_N as

$$M_N = \alpha + \beta m_\pi^2 + \sigma_{NN}(m_\pi, \Lambda) + \sigma_{N\Delta}(m_\pi, \Lambda), \quad (6)$$

by adjusting α, β and Λ to fit the data. Using a sharp cut-off ($u(k) = \theta(\Lambda - k)$) these authors were able to obtain analytic expressions for σ_{NN} and $\sigma_{N\Delta}$ which reveal the correct LNA behaviour – and next to leading (NLNA) in the $\Delta\pi$ case, $\sigma_{N\Delta}^{NLNA} \sim m_\pi^4 \ln m_\pi$. These expressions also reveal a branch point at $m_\pi = M_\Delta - M_N$, which is important if one is extrapolating from large values of m_π to the physical value. The solid curve in Fig. 3 is a two parameter fit to the lattice data using Eq.(6), but fixing Λ at a value suggested by CBM simulations to be equivalent to the preferred 1 GeV dipole. A small increase in Λ is necessary to fit the lowest mass data point (at $m_\pi^2 \sim 0.1 \text{ GeV}^2$) well, but clearly one can describe the data very satisfactorily while preserving the exact LNA and NLNA behaviour of QCD.

The analysis of the lattice data for M_N , incorporating the correct non-analytic behaviour, also yields important new information concerning the sigma commutator of the nucleon:

$$\sigma_N = \frac{1}{3} \langle N | [Q_{i5}, [Q_{i5}, H_{QCD}]] | N \rangle = \langle N | \bar{m}(\bar{u}u + \bar{d}d) | N \rangle, \quad (7)$$

which is a direct measure of chiral SU(2) symmetry breaking in QCD. The widely accepted experimental value is $45 \pm 8\text{MeV}$ [28], although there are recent suggestions that it might be as much as 20 MeV larger [29]. Using the

Feynman-Hellmann theorem one can also write

$$\sigma_N = \bar{m} \frac{\partial M_N}{\partial \bar{m}} = m_\pi^2 \frac{\partial M_N}{\partial m_\pi^2}, \quad (8)$$

at the physical pion mass. Historically, lattice calculations have evaluated $\langle N | (\bar{u}u + \bar{d}d) | N \rangle$ at large quark mass and extrapolated this scale dependent quantity to the “physical” quark mass, which had to be determined in a separate calculation. The latest result with dynamical fermions, $\sigma_N = 18 \pm 5$ MeV [30], illustrates how difficult this procedure is. On the other hand, if one has a fit to M_N as a function of m_π which is consistent with chiral symmetry, one can evaluate σ_N directly using Eq.(8). Using Eq.(6) with a sharp cut-off yields $\sigma_N \sim 55$ MeV, while a dipole form gives $\sigma_N \sim 45$ MeV [31]. The residual model dependence can only be removed by more accurate lattice data at low m_π^2 . Nevertheless, the result $\sigma_N \in (45, 55)$ MeV is in very good agreement with the data. In contrast, the simple cubic fit, with γ inconsistent with chiral constraints, gives ~ 30 MeV. Until the experimental situation regarding σ_N improves, it is not possible to draw definite conclusions regarding the strangeness content of the nucleon from this analysis, but the fact that two-flavour QCD reproduces the current preferred value should certainly stimulate more work.

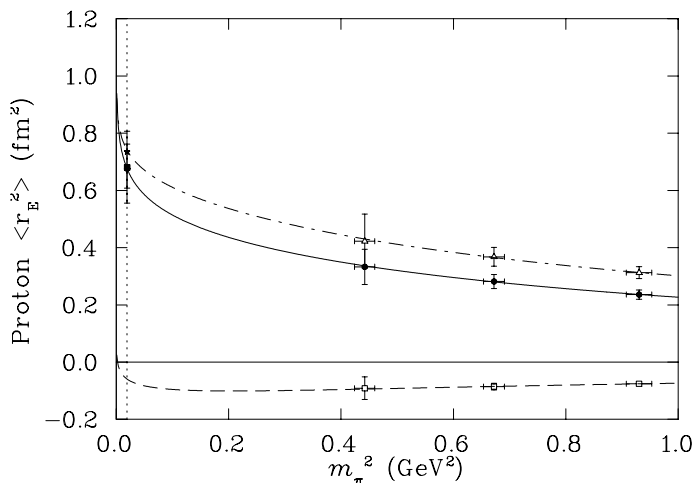


FIGURE 5. Fits to lattice results for the squared electric charge radius of the proton – from Ref. [33]. Fits to the contributions from individual quark flavors are also shown: the u -quark sector results are indicated by open triangles and the d -quark sector results by open squares. Physical values predicted by the fits are indicated at the physical pion mass, where the full circle denotes the result predicted from the first extrapolation procedure and the full square denotes the baryon radius reconstructed from the individual quark flavor extrapolations. (N.B. The latter values are actually so close as to be indistinguishable on the graph.) The experimental value is denoted by an asterisk.

Electromagnetic Properties of Hadrons

It is a completely general consequence of quantum mechanics that the long-range charge structure of the proton comes from its π^+ cloud ($p \rightarrow n\pi^+$), while for the neutron it comes from its π^- cloud ($n \rightarrow p\pi^-$). However it is not often realized that the LNA contribution to the nucleon charge radius goes like $\ln m_\pi$ and diverges as $\bar{m} \rightarrow 0$ [32]. This can never be described by a constituent quark model. Figure 4 shows the latest data from Mainz and Nikhef for the neutron electric form factor, in comparison with CBM calculations for a confinement radius between 0.9 and 1.0 fm. The long-range π^- tail of the neutron plays a crucial role [34, 35].

While there is only limited (and indeed quite old) lattice data for hadron charge radii, recent experimental progress in the determination of hyperon charge radii has led us to examine the extrapolation procedure for obtaining charge data from the lattice simulations [33]. Figure 5 shows the extrapolation of the lattice data for the charge radius of the proton. Clearly the agreement with experiment is much better once the logarithm required by chiral symmetry is correctly included, than if, for example, one simply makes a linear extrapolation in the quark mass (or m_π^2). Full details of the results for all the octet baryons may be found in Ref. [33].

The situation for baryon magnetic moments is also very interesting. The LNA contribution in this case arises from the diagram where the photon couples to the pion loop. As this involves two pion propagators the expansion of the

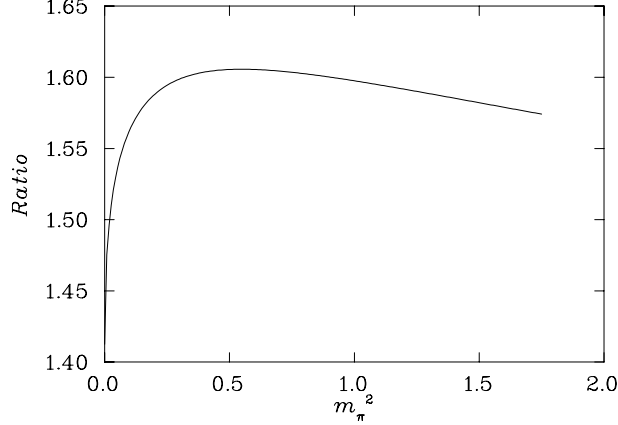


FIGURE 6. Ratio of the (modulus of the) proton to neutron magnetic moments as a function of m_π^2 , obtained from a simple Padé approximant which includes the correct LNA behaviour – from Ref. [42].

proton and neutron moments is:

$$\mu^{p(n)} = \mu_0^{p(n)} \mp \alpha m_\pi + O(m_\pi^2). \quad (9)$$

Here $\mu_0^{p(n)}$ is the value in the chiral limit and the linear term in m_π is proportional to $\bar{m}^{\frac{1}{2}}$, a branch point at $\bar{m} = 0$. The coefficient of the LNA term is $\alpha = 4.4\mu_N\text{GeV}^{-1}$. At the physical pion mass this LNA contribution is $0.6\mu_N$, which is almost a third of the neutron magnetic moment.

Just as for M_N , the chiral behaviour of $\mu^{p(n)}$ is vital to a correct extrapolation of lattice data. One can obtain a very satisfactory fit to some rather old data, which happens to be the best available, using the simple Padé [36]:

$$\mu^{p(n)} = \frac{\mu_0^{p(n)}}{1 \pm \frac{\alpha}{\mu_0^{p(n)}} m_\pi + \beta m_\pi^2} \quad (10)$$

Existing lattice data can only determine two parameters and Eq.(10) has just two free parameters while guaranteeing the correct LNA behaviour as $m_\pi \rightarrow 0$ **and** the correct behaviour of HQET at large m_π^2 . The extrapolated values of μ^p and μ^n at the physical pion mass, $2.85 \pm 0.22\mu_N$ and $-1.90 \pm 0.15\mu_N$ are currently the best estimates from non-perturbative QCD [36]. For the application of similar ideas to other members of the nucleon octet we refer to Ref. [37], and for the strangeness magnetic moment of the nucleon we refer to Ref. [38]. The last example is another case where tremendous improvements in the experimental capabilities, specifically the accurate measurement of parity violation in ep scattering [39, 40, 41], is giving us vital information on hadron structure.

In closing, we note that from the point of view of the naive quark model it is interesting to plot the ratio of the proton to neutron magnetic moments as a function of m_π^2 . The closeness of the experimental value to $-3/2$ is usually taken as a major success. However, we see from Fig. 6 that it is in fact a matter of luck [42]. We stress that the large slope of the ratio near $m_\pi^2 = 0$ is *model independent*.

Moments of Structure Functions

The moments of the parton distributions measured in lepton-nucleon deep inelastic scattering [2] are defined as:

$$\langle x^n \rangle_q = \int_0^1 dx x^n (q(x, Q^2) + (-1)^{n+1} \bar{q}(x, Q^2)), \quad (11)$$

where the quark distribution $q(x, Q^2)$ is a function of the Björken scaling variable x (at momentum scale Q^2). Then the operator product expansion relates these moments to the forward nucleon matrix elements of certain local twist-2 operators which can be accessed in lattice simulations.

Early calculations of moments of structure functions within lattice QCD were performed by Martinelli and Sachrajda [43]. However, the more recent data used in this analysis are taken from the QCDSF [44] and MIT [45] groups and

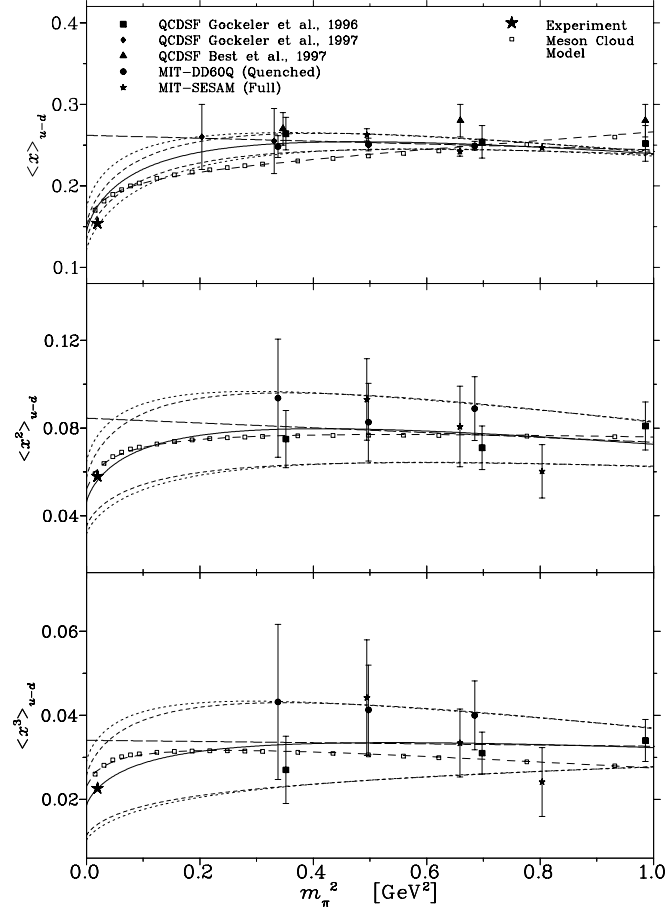


FIGURE 7. Moments of the $u-d$ quark distribution from various lattice simulations. The straight (long-dashed) lines are linear fits to this data, while the curves have the correct LNA behaviour in the chiral limit – see the text for details. The small squares are the results of the meson cloud model and the dashed curve through them best fits using Eq. (13). The star represents the phenomenological values taken from NLO fits in the $\overline{\text{MS}}$ scheme.

shown in Fig. 7 for the $n = 1, 2$ and 3 moments of the $u-d$ difference at NLO in the $\overline{\text{MS}}$ scheme. These calculations have been performed for both full and quenched QCD using a variety of quark actions and for quark masses, \bar{m} , ranging from 50 to 190 MeV.

To compare the lattice results with the experimentally measured moments, one must extrapolate the data from the lowest quark mass used (~ 50 MeV) to the physical value ($\sim 5-6$ MeV). Naively this is done by assuming that the moments depend linearly on the quark mass. However, as shown in Fig. 7 (long dashed lines), a linear extrapolation of the world lattice data for the $u-d$ moments typically overestimates the experimental values by 50%. This suggests that important physics is still being omitted from the lattice calculations and their extrapolations.

Here, as for all other hadron properties, a linear extrapolation in $\bar{m} \sim m_\pi^2$ must fail as it omits crucial nonanalytic structure associated with chiral symmetry breaking. The studies of the chiral extrapolation of lattice data for hadron masses, magnetic moments and charge radii, which we have just reviewed, have shown that for quark masses above 50–60 MeV, hadron properties behave very much as one would expect in a constituent quark model, with relatively smooth behaviour as a function of the quark mass. However, for $\bar{m} < 50$ MeV one typically finds rapid, nonlinear variation arising from the nonanalytic behaviour of Goldstone boson loops [26].

In general, contributions to the physical properties of hadrons from intermediate states involving the surrounding meson cloud give rise to unique terms which are nonanalytic in the quark mass. These stem from the infra-red behaviour of the chiral loops and are *model independent*. The leading nonanalytic (LNA) term for the u and d distributions in the physical nucleon arises from the single pion loop dressing of the bare nucleon and has been shown

[46, 47] to behave as:

$$\langle x^n \rangle_q^{\text{LNA}} \sim m_\pi^2 \log m_\pi. \quad (12)$$

Experience with the chiral behaviour of masses and magnetic moments shows that the LNA terms alone are not sufficient to describe lattice data for $m_\pi > 200$ MeV. Thus, in order to fit the lattice data at larger m_π , while preserving the correct chiral behaviour of moments as $m_\pi \rightarrow 0$, a low order, analytic expansion in m_π^2 is also included in the extrapolation and the moments of $u-d$ are fitted with the form [48]:

$$\langle x^n \rangle_{u-d} = a_n + b_n m_\pi^2 + a_n c_{\text{LNA}} m_\pi^2 \ln \left(\frac{m_\pi^2}{m_\pi^2 + \mu^2} \right), \quad (13)$$

where the coefficient $c_{\text{LNA}} = -(3g_A^2 + 1)/(4\pi f_\pi)^2$ [47]. The parameters a_n , b_n and μ are *a priori* undetermined. The mass μ determines the scale above which pion loops no longer yield rapid variation and corresponds to the upper limit of the momentum integration if one applies a sharp cut-off in the pion loop integral. Multi-meson loops and other contributions cannot give rise to the LNA behaviour in Eq. (12) and thus near the chiral limit Eq. (13) is the most general form for moments of the PDFs at $O(m_\pi^2)$ which is consistent with chiral symmetry.

Having motivated the functional form of the extrapolation formula, we now apply Eq. (13) to the lattice data. Unfortunately, data are not yet available at quark masses low enough to allow a reliable determination of the mass parameter μ . Consequently, for the central curve in each panel of Fig. 7 the value that is most consistent with all experimental moments was chosen, $\mu = 550$ MeV. With μ thus fixed, the results of the best χ^2 fit (for parameters a_n and b_n) to the lattice data for each moment are given by the central solid lines. To estimate the error in the extrapolated value (for a fixed μ), we also fit to the extrema of the error bars on the data as is shown in Fig. 7 by the inner envelopes around these curves.

Experience with other hadronic properties, such as magnetic moments and masses, suggests that the switch (as a function of current quark mass) from smooth and constituent quark-like behaviour (slowly varying with respect to the current quark mass) to rapidly variation (dominated by Goldstone boson loops) happens for $m_\pi \sim 500-600$ MeV. This is very close to the preferred value of μ found here and the similarity of these scales for the various observables simply reflects the common scale at which the Compton wavelength of the pion becomes comparable to the size of the bare hadron. Nevertheless, we stress that μ is not yet determined by the lattice data and it is indeed possible to consistently fit both the lattice data and the experimental values with μ ranging from 400 MeV to 700 MeV. This dependence on μ is illustrated in Fig. 7 by the difference between the inner and outer envelopes on the fits. The former are the best fits to the lower (upper) limits of the error bars, while the latter use $\mu = 450$ (650) MeV instead of the central value of $\mu = 550$ MeV. Data at smaller quark masses, ideally $m_\pi^2 \sim 0.05-0.10$ GeV², are therefore crucial to constrain this parameter and perform an accurate extrapolation.

Baryon Spectroscopy

The study of the baryon spectrum is a venerable art [2]. However, the lack of suitable experimental facilities has meant that there has been insufficient data to provide definitive tests for the many theoretical models constructed over the past 30 years. The availability of high intensity, high duty factor electron accelerators, complemented with multi-particle detectors, means that this situation is changing dramatically. Amongst the open questions to be addressed initially one might ask:

- What is the Roper resonance ($R(1440)$)? In a naive quark model it would be a $2 \not{H}\omega$ excitation of the nucleon, yet it lies below the $1 \not{H}\omega$ negative parity states. Is it a breathing mode [49] or a channel coupling effect [50]?
- Is the $\Lambda(1405)$ a $\bar{K}N$ bound state, as suggested originally by Dalitz and Tuan? Is it a result of the coupling of the $\Sigma\pi-\bar{K}N$ channels, taking into account the extremely attractive $\Sigma\pi$ interaction near threshold [51, 52]?
- Do the missing states, predicted by the quark model but not yet seen experimentally, really exist?
- Are there some states which are not described by the quark model at all, but simply a consequence of very strong rescattering?

We may expect a great deal of experimental insight into these questions in the next few years, from JLab, Mainz and MIT-Bates. At the same time, there are also some exciting developments on the theoretical side. Until now we have had an over-abundance of models, more or less motivated by QCD, with no rigorous way to choose between them. The recent progress in lattice QCD will also have a dramatic impact here. Pioneering work on the $1 \not{H}\omega$ and $2 \not{H}\omega$

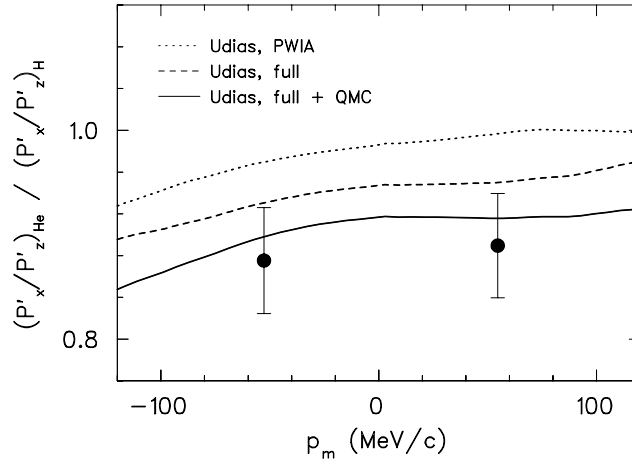


FIGURE 8. Comparison between the ratio of polarised electron quasi-elastic scattering cross sections in ${}^4\text{He}$ and on the free proton. The measured ratio is proportional to the ratio of the proton electric to magnetic form factors of a proton bound in ${}^4\text{He}$ to the ratio for a free proton if the other nuclear effects are correctly handled. The data favour earlier calculations within QMC which predict a change in the bound nucleon form factors. The figure is taken from Ref. [72].

excited states of the nucleon by Leinweber [53], and by Leinweber and Lee [54], is now being developed by at least three groups: at BNL [55], JLab-QCDSF-UKQCD [56] and CSSM [57].

The masses of the $N'(1/2^+)$, $N^*(1/2^-)$, $\Delta^*(3/2^-)$ and even the strange excited states are now being studied in detail with a variety of non-perturbative improvements of the action as well as with domain wall fermions, to improve the chiral properties of the calculation. Again the computer limitations mean that all calculation so far have been quenched and also restricted to relatively large quark mass. Nevertheless some features are already apparent. The data looks very much as one would expect in a constituent quark model. The masses come in the order expected in a simple oscillator picture with $2\hbar\omega$ (positive parity) excitations well above the $1\hbar\omega$ states. Consistent with our earlier summary of the large mass region (\bar{m} above 60MeV), the masses are linear functions of the quark mass. It is clearly vital to extend the calculations to quark masses that are as low as possible and to explore the chiral constraints on the extrapolations of these excited states. There will be tremendous progress in this field in the next five years.

NUCLEAR SYSTEMS

The traditional view of nuclei is as a system of unperturbable (point-like) protons and neutrons. In a mean-field treatment they move in a self-consistent binding potential. Within quantum hadrodynamics (QHD) the Lorentz character of the mean-field is taken seriously, with a strong scalar attraction of order $300\text{--}400\text{ MeV}$ at nuclear matter density (ρ_0) and an almost equally strong vector repulsion [58]. The intermediate range scalar attraction is readily understood in terms of the two-pion-exchange interaction built into the Paris or Bonn potentials, while the vector repulsion involves ω -exchange (possibly with short distance quark exchange). From the point of view of effective field theory this conventional approach is perfectly satisfying and one seeks to determine the additional terms in a complete effective Lagrangian which reproduce all nuclear phenomena [59]. This will involve non-linear meson-baryon couplings and density dependent effective interactions.

On the other hand, believing that we have a complete theory of the strong interactions, namely QCD, it is also fascinating to ask what nuclear phenomena we can understand at that more fundamental level. Indeed, including the transition to a quark-gluon plasma, it is essential to tune one's theoretical ideas at the lower densities of normal nuclei.

If one starts with the aim of understanding nuclear structure in terms of QCD it is fundamental that the protons and neutrons are far from elementary. Indeed, they are quite large composite systems of quarks and gluons. It has been recognized for more than 20 years that the typical nearest neighbour separation at ρ_0 is very close to twice the radius of the nucleon. Furthermore, the typical mean scalar field noted earlier is exactly the same size as the energy required to excite a nucleon (300MeV to the Δ or 500 MeV to the $R(1440)$). **Far from being a surprise that nucleon structure might play a role in nuclear structure, it is difficult to see how it could fail to be significant! One of the central**

aims of modern nuclear physics must be to investigate this role both theoretically and experimentally.

The quest for changes in the structure of hadrons in medium began in the 80's, with considerable attention to the problem being generated by the idea of Brown-Rho scaling [60]. At about the same time, Guichon constructed a simple generalization of QHD, in which the point-like nucleon was replaced by an MIT bag and the σ and ω mesons coupled to the confined quarks [61]. A self-consistent solution of this problem within mean-field approximation led to an astonishing result; the response of the wave function of the confined quarks to the scalar field led to a natural saturation mechanism. That is, rather than the $\sigma - N$ coupling being a constant it becomes a monotonically decreasing function of the applied scalar field, $g_\sigma(\sigma)$. Indeed, because of the low mass of the confined quarks this mechanism is far more effective than the decrease of $\bar{\psi}_N \psi_N$ in QHD, and the mean scalar field at ρ_0 is only 50% or so of that in QHD. Technically, the expression for the energy of nuclear matter in the Guichon model is identical to that in QHD. The only place that the internal structure of the nucleon enters is in the equation for the mean scalar field, where the $\sigma - N$ coupling constant is replaced by $\partial M_N^*/\partial \bar{\sigma}$. The latter **does** depend on the structure of the nucleon – it is essentially its scalar response. Now, this is a quantity which could be calculated on the lattice once one has sufficient control to go to near realistic quark mass. In this way one could actually begin to investigate nuclear saturation with input from QCD itself!

This model, which is generally known as QMC (the quark-meson coupling model), has been extensively developed by Guichon, Saito, Tsushima, Blunden, Miller, Jennings and many others [62, 63, 64, 65]. Exchange contributions have been considered [66] and eventually one must go to a more sophisticated theoretical treatment than simple mean field theory. Nevertheless, the model gives interesting guidance on the modification of hadron masses [67] and reaction cross sections inside nuclear matter [68]. For instance, it provides an interesting alternative to the naive explanation of J/Ψ suppression in relativistic heavy ion collisions in terms of a quark-gluon plasma [69].

From the point of view of nuclear structure the most interesting development is the application to finite nuclei. One can show that, at least at mean-field level, Born-Oppenheimer approximation in which the quark motion adjusts to the local mean-scalar field at any given place, should be good to about 3% for normal nuclei. Then one can derive a nuclear shell model in which the nucleon self-consistently adjusts to the local mean scalar field in each single particle orbital [62]. On the other hand, this derivation implies a **deep conceptual change in our understanding**. What occupies the shell model orbits are not nucleons but nucleon-like quasi-particles. These will have different masses, magnetic moments, charge radii and so on from those of free nucleons. From this point of view is less remarkable that bound nucleons should have different properties from free nucleons than that such changes have proven so difficult to establish. This is why the nuclear EMC effect [71, 70], which is still only partially understood, was so important.

In terms of a fundamental theory of nuclear structure there can be few more important challenges than establishing the change in the properties of a bound nucleon. In this respect, a recent experimental result from Mainz is potentially extremely important [72]. This group used the same triple scattering technique which was so effectively used to determine G_E/G_M for the free proton at JLab, to measure G_E/G_M for a proton bound in ^4He using the $(\vec{e}, e' \vec{p})$ reaction. The change in the ratio of these form factors for the bound nucleon had been studied in detail within QMC [73, 74] and, as shown in Fig. 8, the experimental results support such a modification. Clearly the statistical significance of the effect is not yet great. On the other hand, careful theoretical study of the effects of distortion, spin-orbit forces and meson exchange suggests that this particular ratio is extremely insensitive to such corrections. This measurement is crucial in that it is really the first clear indication of a change in the structure of a bound nucleon. It will stimulate a great deal more work!

CONCLUSION

This is indeed an exciting period in the development of hadron physics. We have seen that developments in lattice QCD, especially more powerful computers and improved chiral extrapolations, should finally allow the computation of accurate hadron properties within full QCD, *at the physical quark masses*, within the next five years. We can also expect new insights into the structure of the QCD vacuum, the nature of confinement and the mechanism for spontaneous chiral symmetry breaking. Studies of hadron spectroscopy on the lattice will complement important new experimental studies and improved quark models.

We have seen that from the point of view of QCD, it is vital to understand the changes in hadron properties that occur as a function of density as well as temperature. In this sense finite nuclei provide a crucial testing ground for ideas that will eventually be applied at much more extreme conditions. Crucial experiments involve the possible binding of ω , η and even charmed mesons in finite nuclei, as well as the changes in the form factors of bound nucleons expected within

QCD and predicted within various QCD motivated models. We briefly reviewed an experiment that gives a tantalizing hint of such a change and look forward to the many further tests of these ideas that will follow in the next few years.

ACKNOWLEDGMENTS

It is a pleasure to acknowledge the contributions from many collaborators in the development of the ideas presented here. I would especially like to thank my colleagues at CSSM and particularly Derek Leinweber, Wally Melnitchouk and Tony Williams. This work was supported by the Australian Research Council and the University of Adelaide.

REFERENCES

1. H. Toki and H. Suganuma, *Prog. Part. Nucl. Phys.* **45**, S397 (2000).
2. A. W. Thomas and W. Weise, "The Structure of the Nucleon," 289 pages. *Hardcover ISBN 3-527-40297-7 Wiley-VCH, Berlin 2001.*
3. V. A. Novikov, M. A. Shifman, A. I. Vainshtein and V. I. Zakharov, *Nucl. Phys. B* **191**, 301 (1981).
4. G. 't Hooft, *Phys. Rev. D* **14**, 3432 (1976) [Erratum-ibid. *D* **18**, 2199 (1976)].
5. <http://hermes.physics.adelaide.edu.au/theory/staff/leinweber/VisualQCD/QCDvacuum/index.html>
6. F. D. Bonnet, D. B. Leinweber, A. G. Williams and J. M. Zanotti, hep-lat/0106023.
7. P. C. Tandy, *Prog. Part. Nucl. Phys.* **36**, 97 (1996) [nucl-th/9605029].
8. C. D. Roberts and A. G. Williams, *Prog. Part. Nucl. Phys.* **33**, 477 (1994) [hep-ph/9403224].
9. R. Alkofer and M. Oettel, "Nucleon form factors in the covariant diquark-quark model," hep-ph/0105320.
10. F. D. Bonnet, P. O. Bowman, D. B. Leinweber, A. G. Williams and J. M. Zanotti, *Phys. Rev. D* **64**, 034501 (2001) [hep-lat/0101013].
11. R. Alkofer and L. von Smekal, *Nucl. Phys. A* **680**, 133 (2000) [hep-ph/0004141].
12. F. T. Hawes, P. Maris and C. D. Roberts, *Phys. Lett. B* **440**, 353 (1998) [nucl-th/9807056].
13. S. Aoki *et al.* [JLQCD Collaboration], *Phys. Rev. Lett.* **82** (1999) 4392.
14. J. Skullerud, D. B. Leinweber and A. G. Williams, hep-lat/0102013.
15. E. I. Ivanov *et al.* [E852 Collaboration], *Phys. Rev. Lett.* **86**, 3977 (2001) [hep-ex/0101058].
16. P. Lacock and K. Schilling [SESAM collaboration], *Nucl. Phys. Proc. Suppl.* **73**, 261 (1999) [hep-lat/9809022].
17. C. Bernard *et al.* [MILC Collaboration], *Phys. Rev. D* **56**, 7039 (1997) [hep-lat/9707008].
18. A. Dzierba *et al.*, *Hall D Collaboration Preliminary Design Report ver. 3*, <http://dustbunny.physics.indiana.edu/HallD/>
19. C. Michael, "Glueballs, hybrid and exotic mesons," hep-ph/0101287.
20. D. V. Bugg, *Nucl. Phys. Proc. Suppl.* **96**, 218 (2001).
21. D. B. Leinweber, A. W. Thomas, K. Tsushima and S. V. Wright, *Phys. Rev. D* **61**, 074502 (2000) [hep-lat/9906027].
22. T. Lippert, S. Gusken and K. Schilling, *Nucl. Phys. Proc. Suppl.* **83** (2000) 182.
23. S. Aoki *et al.* [CP-PACS-Collaboration], *Phys. Rev. D* **60**, 114508 (1999) [hep-lat/9902018].
24. S. Theberge, A. W. Thomas and G. A. Miller, *Phys. Rev. D* **22**, 2838 (1980) [Erratum-ibid. *D* **23**, 2106 (1980)]; A. W. Thomas, *Adv. Nucl. Phys.* **13**, 1 (1984).
25. Lattice Hadron Physics Collaboration proposal, "Nuclear Theory with Lattice QCD", J.W. Negele and N. Isgur principal investigators, March 2000, <ftp://www-ctp.mit.edu/pub/negele/LatProp/>.
26. S. Weinberg, *Physica (Amsterdam)* **96 A**, 327 (1979); J. Gasser and H. Leutwyler, *Ann. Phys.* **158**, 142 (1984).
27. C. R. Allton *et al.* [UKQCD Collaboration], *Phys. Rev. D* **60**, 034507 (1999) [hep-lat/9808016].
28. J. Gasser, H. Leutwyler and M. E. Sainio, *Phys. Lett. B* **253**, 252 (1991).
29. M. Knecht, *PiN Newslett.* **15**, 108 (1999) [hep-ph/9912443].
30. S. Gusken *et al.* [SESAM Collaboration], *Phys. Rev. D* **59**, 054504 (1999) [hep-lat/9809066].
31. S. V. Wright, D. B. Leinweber and A. W. Thomas, *Nucl. Phys. A* **680**, 137 (2000) [nucl-th/0005003].
32. D. B. Leinweber and T. D. Cohen, *Phys. Rev. D* **47**, 2147 (1993) [hep-lat/9211058].
33. E. J. Hackett-Jones, D. B. Leinweber and A. W. Thomas, *Phys. Lett. B* **494**, 89 (2000) [hep-lat/0008018].
34. D. H. Lu, S. N. Yang and A. W. Thomas, *Nucl. Phys. A* **684**, 296 (2001).
35. D. H. Lu, A. W. Thomas and A. G. Williams, *Phys. Rev. C* **57**, 2628 (1998) [nucl-th/9706019].
36. D. B. Leinweber, D. H. Lu and A. W. Thomas, *Phys. Rev. D* **60**, 034014 (1999) [hep-lat/9810005].
37. E. J. Hackett-Jones, D. B. Leinweber and A. W. Thomas, *Phys. Lett. B* **489**, 143 (2000) [hep-lat/0004006].
38. D. B. Leinweber and A. W. Thomas, *Phys. Rev. D* **62**, 074505 (2000) [hep-lat/9912052].
39. D. T. Spayde *et al.* [SAMPLE Collaboration], proton's strange magnetic form-factor," *Phys. Rev. Lett.* **84**, 1106 (2000) [nucl-ex/9909010].
40. K. S. Kumar and P. A. Souder, *Prog. Part. Nucl. Phys.* **45**, S333 (2000).
41. P. A. Souder [HAPPEX Collaboration], *Nucl. Phys. A* **663**, 939 (2000).
42. D. B. Leinweber, A. W. Thomas and R. D. Young, *Phys. Rev. Lett.* **86**, 5011 (2001) [hep-ph/0101211].

43. G. Martinelli and C. T. Sachrajda, Phys. Lett. B **196**, 184 (1987).
44. M. Gockeler, R. Horsley, E. M. Ilgenfritz, H. Perlt, P. Rakow, G. Schierholz and A. Schiller, Nucl. Phys. Proc. Suppl. **53**, 81 (1997) [hep-lat/9608046].
45. D. Dolgov *et al.*, Nucl. Phys. Proc. Suppl. **94**, 303 (2001) [hep-lat/0011010].
46. A. W. Thomas, W. Melnitchouk and F. M. Steffens, Phys. Rev. Lett. **85**, 2892 (2000) [hep-ph/0005043].
47. D. Arndt and M. J. Savage, "Chiral Corrections to Matrix Elements of Twist-2 Operators," nucl-th/0105045; J. Chen and X. Ji, hep-ph/0105197.
48. W. Detmold, W. Melnitchouk, J. W. Negele, D. B. Renner and A. W. Thomas, hep-lat/0103006, to appear in Phys. Rev. Lett. (2001).
49. P. A. Guichon, Phys. Lett. B **163**, 221 (1985).
50. J. Speth, O. Krehl, S. Krewald and C. Hanhart, Nucl. Phys. A **680**, 328 (2000).
51. E. A. Veit, B. K. Jennings, A. W. Thomas and R. C. Barrett, Phys. Rev. D **31**, 1033 (1985).
52. N. Kaiser, P. B. Siegel and W. Weise, Nucl. Phys. A **594**, 325 (1995) [nucl-th/9505043]; E. Oset, A. Ramos and C. Bennhold, "Low lying $S = -1$ excited baryons and chiral symmetry," arXiv:nucl-th/0109006.
53. D. B. Leinweber, Phys. Rev. D **51**, 6383 (1995) [nucl-th/9406001].
54. F. X. Lee and D. B. Leinweber, Nucl. Phys. Proc. Suppl. **73**, 258 (1999) [hep-lat/9809095].
55. S. Sasaki, T. Blum and S. Ohta, "A lattice study of the nucleon excited states with domain wall fermions," hep-lat/0102010.
56. M. Gockeler, R. Horsley, D. Pleiter, P. E. Rakow, G. Schierholz, C. M. Maynard and D. G. Richards [QCDSF Collaboration], "Negative-parity baryon masses using an O(a)-improved fermion action," hep-lat/0106022.
57. J. Zanotti *et al.*, in preparation.
58. R. J. Furnstahl and B. D. Serot, Comments Nucl. Part. Phys. **2**, A23 (2000) [nucl-th/0005072].
59. B. D. Serot and J. D. Walecka, nucl-th/0010031.
60. G. E. Brown and M. Rho, Phys. Rev. Lett. **66**, 2720 (1991).
61. P. A. Guichon, Phys. Lett. B **200**, 235 (1988).
62. P. A. Guichon, K. Saito, E. N. Rodionov and A. W. Thomas, Nucl. Phys. A **601**, 349 (1996) [nucl-th/9509034].
63. K. Saito, K. Tsushima and A. W. Thomas, Phys. Rev. C **55**, 2637 (1997) [nucl-th/9612001].
64. P. G. Blunden and G. A. Miller, Phys. Rev. C **54**, 359 (1996) [nucl-th/9602031].
65. X. Jin and B. K. Jennings, Phys. Rev. C **54**, 1427 (1996) [nucl-th/9604018].
66. G. Krein, A. W. Thomas and K. Tsushima, Nucl. Phys. A **650**, 313 (1999) [nucl-th/9810023].
67. K. Tsushima, D. H. Lu, A. W. Thomas and K. Saito, Phys. Lett. B **443**, 26 (1998) [nucl-th/9806043].
68. K. Tsushima, A. Sibirtsev and A. W. Thomas, J. Phys. G **G27**, 349 (2001) [nucl-th/0008039].
69. A. Sibirtsev, K. Tsushima, K. Saito and A. W. Thomas, Phys. Lett. B **484**, 23 (2000) [nucl-th/9904015].
70. D. F. Geesaman, K. Saito and A. W. Thomas, Ann. Rev. Nucl. Part. Sci. **45**, 337 (1995).
71. J. J. Aubert *et al.* [European Muon Collaboration], Deuterium," Phys. Lett. B **123**, 275 (1983).
72. S. Dieterich *et al.*, Phys. Lett. B **500**, 47 (2001) [nucl-ex/0011008].
73. D. H. Lu, K. Tsushima, A. W. Thomas, A. G. Williams and K. Saito, Phys. Rev. C **60**, 068201 (1999) [nucl-th/9807074].
74. A. W. Thomas, D. H. Lu, K. Tsushima, A. G. Williams and K. Saito, nucl-th/9807027.